TW3-TPP-ERDIAG

Task Title: EVALUATION OF LASER ABLATION OPTICAL EMISSION SPECTROSCOPY (LA-OES) METHOD FOR GRAPHITE CO-DEPOSITED LAYER CHARACTERIZATION

INTRODUCTION

In-situ diagnostics of the plasma facing surface is regarded crucial for fusion investigations. A further development of the diagnostics is seen essential in dealing with erosion and deposition in nuclear fusion experiments. The application of new materials such as beryllium (instead of graphite) and carbon fibre composite (CFC) requires also further improvement and development of the diagnostics. It should be stressed that the available diagnostics can not completely explain the matter transport from plasma to the component surface in modern TOKAMAK reactors. Within the frames of our investigations on laser detritiation [1-2], some ablation and thermal measurements were made and analysed. The rigid nuclear safety rules in working with tritium and beryllium limited the investigations. Thus, the laboratory measurements were made only with a few available samples of TexTor and TORE SUPRA graphite.

Laser Ablation Optical Emission Spectroscopy (LA-OES) diagnostics (in some publications referred as LIBS - Laser Induced Breakdown Spectroscopy) was under study. The possibility to make in-situ completely optical measurements inside the vacuum chamber is regarded as an advantage of this method. LA-OES is applied for a surface quantitative or qualitative elemental analysis. The analysis allows to detect the atomic lines emitted by plasma induced after the nanosecond laser pulse interaction with the surface. Generally, LA-OES is applied with the nearly Gaussian laser beam [3-4]. The craters are conical. Each laser pulse results in a sample ablation from different depths. This paper demonstrates that it is possible to use a "homogeneous" laser beam to form cylindrical craters when each laser pulse ablates the sample from a definite depth. The possible LA-OES application to determine both the composition and the thickness of a co-deposited layer was under investigation. In our experiments, thin (up to 10 μm) and thick (50 μm) layers were studied. Our previous experiments [5] demonstrated that LA-OES allows to detect certain impurities of a co-deposited layer. The development of the diagnostics to analyse the hydrogen and the impurities contents in a co-deposited layer was the aim of our recent investigations. Hydrogen contents measurements are of the fundamental importance for future TOKAMAK (ITER). The hydrogen Balmer series line (n=3 → n=2) in the visible spectral range at 656 nm was observed and detected. The isotopic shift between hydrogen and deuterium line is 0.2 nm. As H-line width was ≈ 2 nm (a full width at half maximum), it was not possible to distinguish hydrogen isotopes. The energy of the upper transition level is ≈12 eV. Thus, it was necessary to create hot plasma on the sample by high laser fluence.

2004 ACTIVITIES

LA-OES method in application to graphite tile with a co-deposited layer was studied on the DPC/SCP/LRSI installation (figure 1) that was modified and adjusted for graphite co-deposited layer investigations. The second harmonic (532 nm, 6 ns) of Nd-YAG laser (Brillant, Quantel) was focused onto the surface by the lens (100 mm or 250 mm focal length). The laser pulse energy was ≈ 60 mJ (without the diaphragm 2) and ≈ 20 mJ (with the diaphragm 2). The diaphragms were applied to homogenise the laser beam intensity distribution that was hyper-Gaussian with 2.5 rad beam divergence. The diameters of the diaphragm 1 and diaphragm 2 were 6 mm and 3 mm, respectively. A graphite sample was placed in a specially developed sealed sell to protect (especially, against the oxygen molecules) the treated surface and laser plasma by argon. The cell was filled with argon, 1 bar pressure. Two optical fibers were used to collect the plasma light and to transport it to the spectrometer entrance slits.

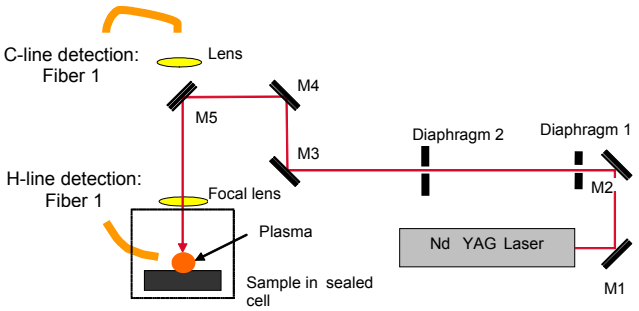

Figure 1 : LA-OES installation

The spectral analysis of the laser plasma plume was made with two 1-meter focal length Czerny Turner spectrometers (Acton Research and THR 1000, Jobin Yvon) supplied with ICCD cameras (ICCD I Max, Roper Scientific) to detect the time resolved spectral line intensity. One spectrometer was adjusted to detect carbon CI-line ($\lambda = 247.856$ nm, $E_k = 7.685$ eV, $g_i = 1$, $g_k = 3$, $A_{ki} = 0.34 \times 10^8$ s^{-1}), while the other – for hydrogen line detection ($\lambda \cong 656.281$ nm, 656,274 nm and 656,286 nm, $E_k \cong 12.088$ eV, $g_i = 6$, $g_k = 16$, $A_{ki} = (0.696 + 0.435 + 0.0014) \times 10^8$ s^{-1}).

The experiments with non-homogeneous laser beam and high (40-100 J/cm^2) laser fluence were performed with 60 mJ laser beam (without the diaphragm 2). The beam was focused onto the TexTor graphite surface by the lens (100 mm focal length) in 0.25-0.4 mm diameter spot to provide 40-100 J/cm^2 laser fluence on the sample. 1200 laser shots were applied for one crater ablation in air at 1 bar pressure.

The laser spot diameter on the target was estimated as $D_L \approx \Theta_L \times F \approx 0.0025$ rad × 100mm = 0.25 mm, where Θ_L is the laser beam angular divergence. After the graphite surface ablation with 1200 pulses, the crater diameter on the sample surface was determined as 0.4 mm. The "conical" crater depth was 0.35 mm or higher. The spectral line intensities of hydrogen (656.2852 nm), carbon (247.856 nm), and also of some impurities (B, Si, and Fe) were detected for each laser pulse. The ICCD cameras with 1 μs delay and 10 μs gate time were chosen for application. The spectral line intensities (as a function of the number of the applied pulses) decreased and vanished after 150 pulses application for impurities (B, Si and Fe) and after 300-400 pulses for H and C.

The experiments with non-homogeneous laser beam and medium (20-26 J/cm^2) laser fluence were performed with two diaphragms (figure 1). Diaphragm 2 was placed at the distance s_1 = 1250 mm from the focusing lens with the focal length F = 250 mm. The sample was placed in the lens F focal position. Six craters were formed after 1200 pulses. Laser ablation rate was of 0.5 μm per pulse. The face surface with a co-deposited layer and the backside surface of TexTor tile were under study. 1200 analytical spectra were detected for each crater. For the typical crater diameters of 300-400 μm that were determined with the mechanical profilometer and the optical microscope, the laser spot surface was ≈ 0.001 cm^2. The optical microscope observations confirmed the "conical" crater shape. Spectral line measurements were performed with ICCD camera 10 μs gate time, 0.1 μs delay for H and 0.8 μs delay for C**.** The typical laser plasma spectra with hydrogen, carbon, and impurity lines are presented (figure 2 and figure 3).

The hydrogen and carbon lines were observed over ≈600 pulses. The ratio of H/C line intensities for face and backside TexTor tile surfaces are presented on figure 4 and figure 5. The H/C line intensity ratio is high (3÷6) for the face surface with a co-deposited layer during 30 pulses.

Then, the H/C ratio deceases to a constant value 1.5 and 1 for the face and backside surface, respectively. The B, Fe, Si, and Cu impurity traces were detected during ≈ 3 pulses for the backside surface and during ≈ 300 pulses for the face surface.

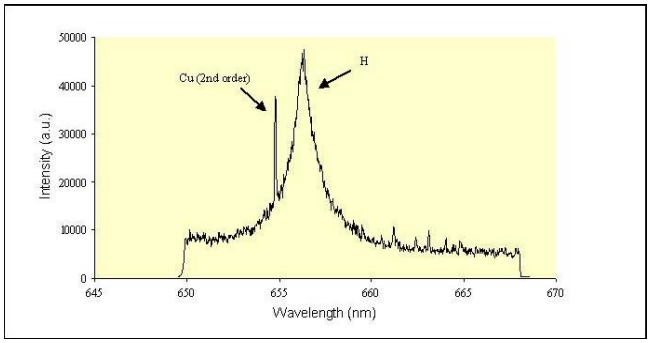

Figure 2 : Typical spectrum in the red range. Gain of ICCD - 255, delay - 0.1 μs, gate time - 10 μs, one crater, 1200 spectra were accumulated

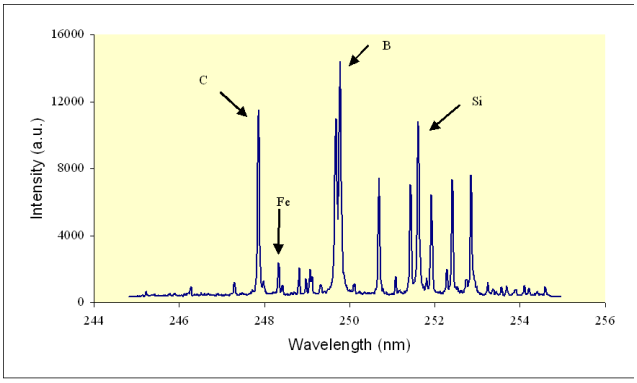

Figure 3 : Typical spectrum in the VU range. Gain of ICCD - 160 ; Delay - 0.8 μs ; Gate time - 10 μs ; one crater; 1200 spectra were accumulated.

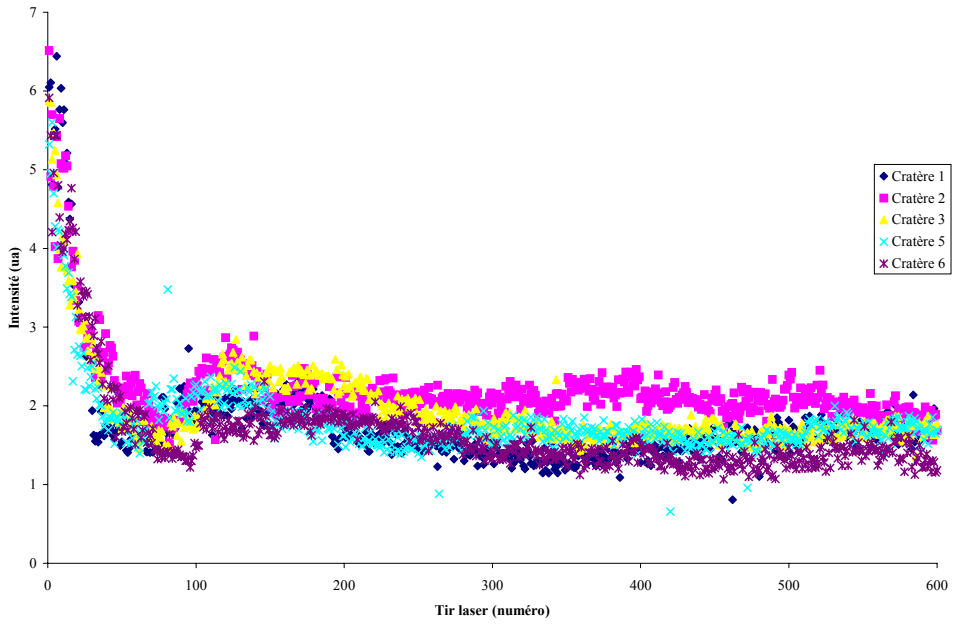

Figure 4 : The ratio of H/C line intensities for six craters on the face surface (with a co-deposited layer) as a function of the pulse number

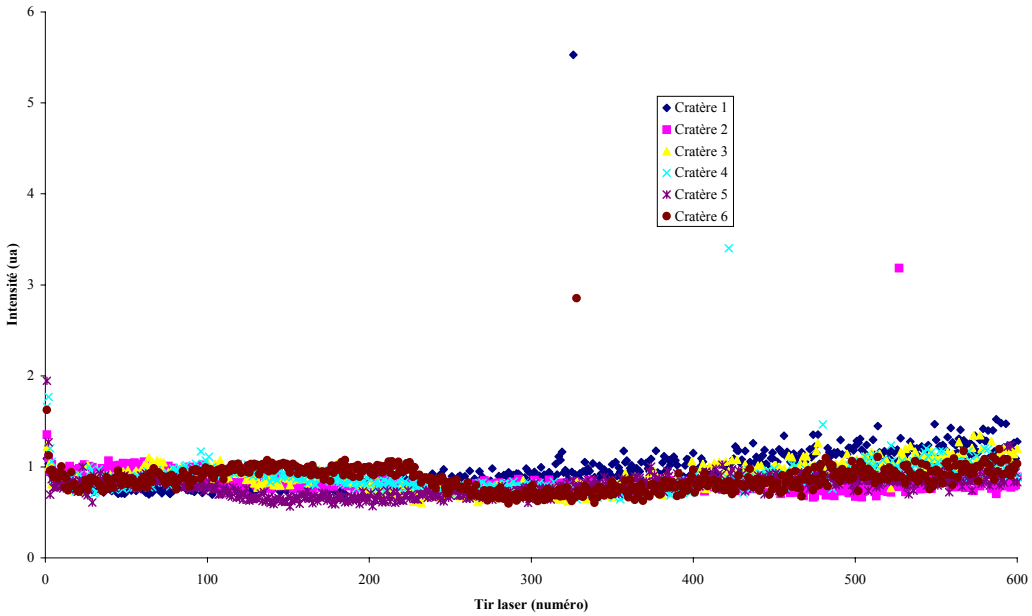

Figure 5 : The ratio of H/C line intensities for six craters on the backside surface (without a co-deposited layer) as a function of the pulse number

The experiments with "homogeneous" laser beam and low (4.5 J/cm^2) laser fluence were performed with the diaphragm 2 aperture (D_2=3mm diameter) being imaged on the sample (TexTor graphite with and without a co-deposited layer). The graphite sample was placed at the distance $b=s/[(s/F)-1]$ from the lens F. For F = 250 mm and s = 1250 mm, the distance b = 312.5 mm. In this case, the laser spot diameter on the graphite sample is $D_s=D_2/[(s/F)-1]$ = 750μm that corresponds to the laser spot surface 0.25 π $D_s^2 \cong 4.4 \times 10^{-3}$ cm^2. For the laser energy E ≅ 20 mJ, the laser fluence was 4.5 J/cm^2. In this case, the spectral line intensities were very weak or undetectable.

To avoid the effect of the atmospheric water hydrogen (vapour water molecules can dissociate in laser plasma and result in the atomic hydrogen), a sealed cell with argon was developed. It was used to study LA-OES spectral lines in neutral atmosphere. The experiments with "homogeneous" laser beam and medium (20 J/cm^2) laser fluence were performed with the sealed cell with argon under 1 bar pressure. 13 mJ laser pulse energy was applied. The 3 mm diameter diaphragm 2 was placed at 2250 mm from the focusing lens F = 250 mm.

The sample surface was at 235 mm from the focusing lens. The graphite ablation rate was ≈ 0.25 μm per pulse. Figure 6 presents a crater form obtained with "homogeneous" laser beam for Al-target with a relatively low surface roughness.

The experimental parameters were as follows: the ICCD camera gate time - 10 μs, the delay - 0.4 μs for carbon spectral line detection, and 0.1 μs for hydrogen spectral line. 600 spectra were detected for each crater. The argon gas application resulted mainly in the spectral line intensities increase. Both in air and in argon, the H/C ratio and line intensity changes with the pulse number were almost the same.

Thus, the application of argon environment should not be considered critical for the co-deposited layer analysis. The argon application manifested itself as a black re-deposition around the craters. The black circular zone was not detected with ablation in air, but was observed in Ar. It is considered to be resulting from the graphite powder re-deposition. The graphite powder appeared in the laser plasma plume after its cooling and condensation into micro particles. Ar was keeping hydrogen atoms from oxidation. In air, oxygen gave rise to CO_2 and, thus, suppressed the black circle formation around the crater.

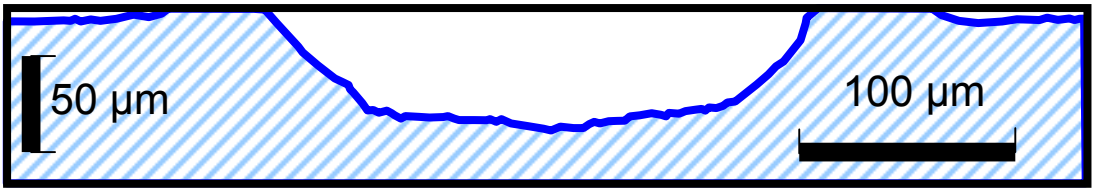

Figure 6 : Crater form obtained with "homogeneous" laser beam on Al-target

CONCLUSIONS

To study LA-OES specific applications to graphite co-deposited layer, a special laser installation was developed and implemented. The installation was used to make time resolved spectral measurements on laser plasma in the controlled environment (argon or air). The experiments with high and medium laser fluence demonstrated the necessity "to homogenise" the laser beam.

The analytical transition wavelengths for hydrogen, carbon, and other impurities (B, Fe, Si, Cu) were determined. For LA-OES measurements, a sufficiently high laser fluence (10-20 J/cm^2) was required. This requirement resulted from a high energy of the analytical transition of the upper levels for hydrogen (12 eV) and carbon (7.7 eV).

Hydrogen was detected on two sides of the TexTor tile samples (with and without co-deposited layer). In our experiments, hydrogen was detected even in the bulk graphite (for 100- 1000 pulse range). The H/C spectral line intensity ratios were different for face and backside surfaces. The hydrogen spectral line intensity was higher on the surface with a co-deposited layer. On a thick co-deposited layer, the H/C ratio was observed up to 30 pulses. The significant H/C ratio was observed only for the initial 5 pulses on a backside surface on a thin co-deposited layer.

A sealed cell with argon was developed and implemented to study LA-OES spectral lines in neutral atmosphere. The argon gas application resulted in the spectral line intensities increase. The H/C ratio and line intensity changes with the pulse number were practically the same both in air and argon. The argon effect manifested itself as a black re-deposition around the craters. The black circular zone was observed in Ar, but was not detected with ablation in air.

The results of our investigations should be regarded rather optimistic for in-situ LA-OES applications in fusion reactors. On the basis of the obtained results, certain ways to improve the LA-OES analytical performances are envisaged. Thus, the study on LA-OES future improvement and optimization (LA with homogeneous beam of 20 J/cm^2 laser fluence, LA-OES with ultra short laser pulses [6], two pulse plasma reheating [7], etc.) should be considered important.

REFERENCES

[1] A. Semerok et al. - Studies on graphite surfaces detritiation by pulsed repetition rate nanosecond lasers - CEA report NT DPC/SCP/04-076-A, 2004, pp. 39.

[2] A. Semerok et al. - Studies on TOKAMAK wall surfaces deconamination by pulsed repetition rate lasers - CEA report NT DPC/SCP/05-111-A, 2005, pp.50.

[3] C. Geertsen et al, Spectrochemica Acta, B 51, (1996) 1403-1416

[4] B. Sallé et al, Spectrochemica Acta, B-59 (2004) 1413-1422.

[5] F. Le Guern et al., J. Nucl. Material, 335 (2004) 410-416.

[6] A. Semerok et al, Laser and Particle Beams. 20, (2002), 67-72.

[7] A. Semerok, Ch. Dutouquet, Thin Solid Films, 435-434 (2004) 501-505.

TASK LEADER

Alexandre SEMEROK

DEN/DPC/SCP/LILM
CEA-Saclay
F-91191 Gif-sur-Yvette Cedex

Tél. : 33 1 69 08 65 57
Fax : 33 1 69 08 78 84

E-mail : asemerok@cea.fr

CEFDA01-645

Task Title: TW2-TPHN-NBDES1: SUPPORT TO NEUTRAL BEAM PHYSICS AND TESTING 1

INTRODUCTION

The European concept for a 1 MeV, 40 A negative ion based accelerator for the neutral beam system on ITER, the SINgle GAP, SINGle Aperture (SINGAP), is an attractive alternative to the ITER reference design, the so-called Multi-Aperture, Multi-Grid (MAMuG) accelerator. A prototype SINGAP accelerator has been used for several years and produced D^- beams with an energy of 910 keV, 60 A/m^2 simultaneously [1]. The measured beam profiles on the target agree well with the ones predicted by beam optics calculations [2]. However with this prototype accelerator it was not possible to produce beams with optics acceptable to ITER. Therefore a new accelerator, the "ITER-like" accelerator, has been built in order to demonstrate that the beam optics required for ITER can be achieved [3]. A new ion source has also been built which is fully water cooled to allow repetitive pulsing at the required power levels.

2004 ACTIVITIES

THE NEW ITER-LIKE ACCELERATOR AND THE NEW ION SOURCE

The new ion source is a revised version of the earlier prototype "Drift Source" [4]. The source is mounted inside the vacuum. The side plates are made by Cu deposition and contain water cooling channels and the CoSm magnets which provide the fast electron confinement.

The top, bottom and back plates are made of water cooled OFHC copper. They contain no magnets and the cooling water channels were created by deep drilling.

The pre-accelerator consists of a plasma grid, an extraction grid and a pre-acceleration grid. Each grid is mounted on a circular stainless steel (SS) grid support plate. Each support plate is supported on alumina post insulators from a common SS base plate. The extraction grid and the pre-acceleration grid have aperture patterns of 5 x 5 with a horizontal and vertical pitch of 20 mm. A 20 mm high "kerb" made of stainless steel is fitted at the exit of the pre-accelerator.

This kerb modifies the electric field such that the outer beamlets are "pushed" towards the beam centre in order create adequately parallel beamlets at the exit of the post-accelerator.

Four different plasma grids have been made, with the number of apertures varying from 3 to 25. The Cadarache 1 MV power supply has a current limit of 100 mA. This limits the numbers of apertures on the plasma grid to three when 200 A/m^2, 1 MeV beams are to be produced.

However, for comparison of experiment and modelling it is more suitable to use rows of 5 apertures and reduce the beam energy. The plasma grid with 25 apertures will be used when the SINGAP accelerator will be tested at the megavolt test stand at JAERI, Naka in Japan in the near future, where a 1 MV – 1 A power supply is available.

A cross section of the "ITER-like" accelerator with the ion source can be seen in figure 1.

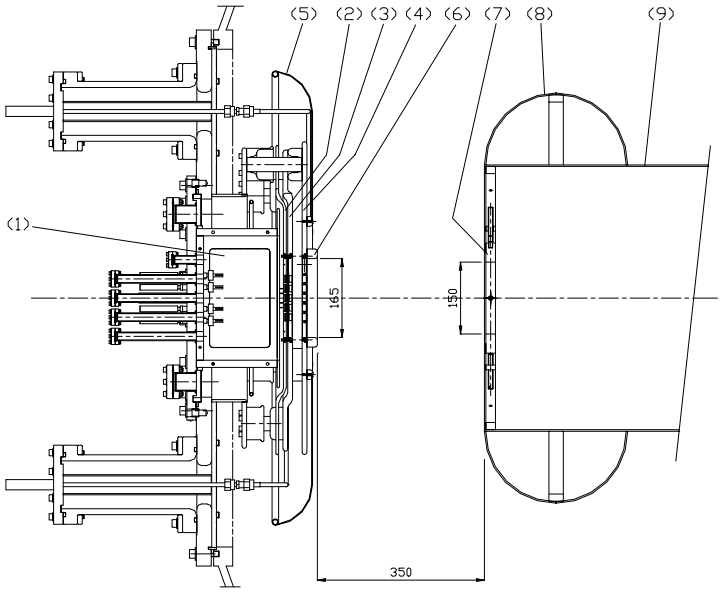

(1) 'Drift Source'
(2) plasma grid support (~10 V)
(3) extraction grid support (<+10 kV)
(4) pre-acceleration grid support (<+50 kV)
(5) electrostatic screen
(6) electrostatic "kerb" structure
(7) post-accelerator electrode (+1 MV)
(8) electrostatic stress ring
(9) drift tube

Figure 1 : Vertical section of the "ITER-like" SINGAP Beam Source

The 4 plasma grids have each two heater elements embedded in the source side of the grids to enable heating of the plasma grid to ≈ 300 °C for efficient negative ion production with Cs seeding of the source [5].

The extraction grid and the pre-acceleration grid are both water cooled through horizontal channels between the aperture rows and incorporate CoSm magnets for electron suppression and/or ion trajectory correction. Since the grids are rather complex they were manufactured using electrolytic Cu deposition.

The beamlets formed in the pre-accelerator are accelerated to an energy of 1 MeV in one step across the main acceleration gap of 350 mm. The post-accelerator electrode has only one large square opening and is made of OFHC Cu. It can be displaced vertically and horizontally, thus providing aperture offset beam steering to simulate the vertical steering (± 0.55°) required on ITER or for correcting for beam misalignment.

Both the pre-accelerator and the post-accelerator have been provided with electro-polished SS screens to reduce the electrostatic stresses and they are arranged to ensure that the beam optics is not influenced by fringe fields.

VOLTAGE HOLDING

Breakdown free HV pulses up to 940 kV were achieved after only 160 minutes of accumulated voltage on-time. Helium gas with a pressure of about 0.05 Pa was added into the vacuum tank in order to suppress dark currents [6]. Higher voltages have not been attempted in order to minimise the risk of damaging the 1 MV power supply.

BEAM OPTICS SIMULATIONS

The first comparisons between simulations and experiments have been done for SINGAP in the ITER-like configuration. Shot 7545 was chosen for the simulation because the the three beamlets are well resolved, which facilitates the detailed comparison with the simulations.

Shot 7545 had 1.8 s of 28 A/m^2 D$^-$ beams, 13 mA in total, as determined from the energy deposited onto the 19 mm thick Mitsubishi MFC 1A graphite target.

Taking stripping losses into account, the extracted current density from the source was 36 A/m^2.

The extraction voltage was 2.5 kV, the pre-acceleration voltage 18 kV and the post-acceleration voltage 625 kV.

The source pressure was 0.4 Pa, the plasma grid was at 225 °C and caesium was introduced. The result of the simulation can be seen on the right in figure 2.

The simulation procedure is described in detail in [2]. An addition to the previously described procedure is that the calculated temperature profiles are now corrected for the time and temperature dependent 3D heat diffusion occurring during the transit from the exposed front towards the rear face of the carbon target where the temperature distribution is measured experimentally.

EXPERIMENTAL DATA

The measured infra red data is shown on the left in figure 2 and on the right, the calculated power density as seen from the back of the target.

We see from the data in figure 2:

- The two beamlets on the right are vertically 30 mm apart (the calculation gives 23 mm).
- The lower two beamlets are horizontally 11 mm apart (the calculation gives 12 mm).
- The power density profile is wider than calculated, but the central part not by very much.

The reason why the beamlets are vertically further apart than calculated is not yet clear.

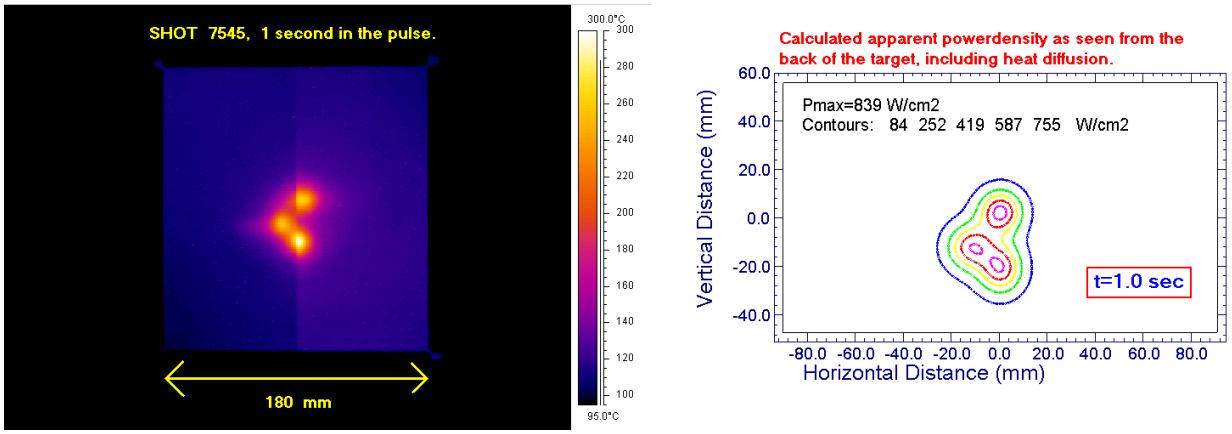

Figure 2 : Infra red data taken from the back of the carbon target for shot 7545 (28 A/m^2 D$^-$) is shown on the left The calculated power density is shown on the right

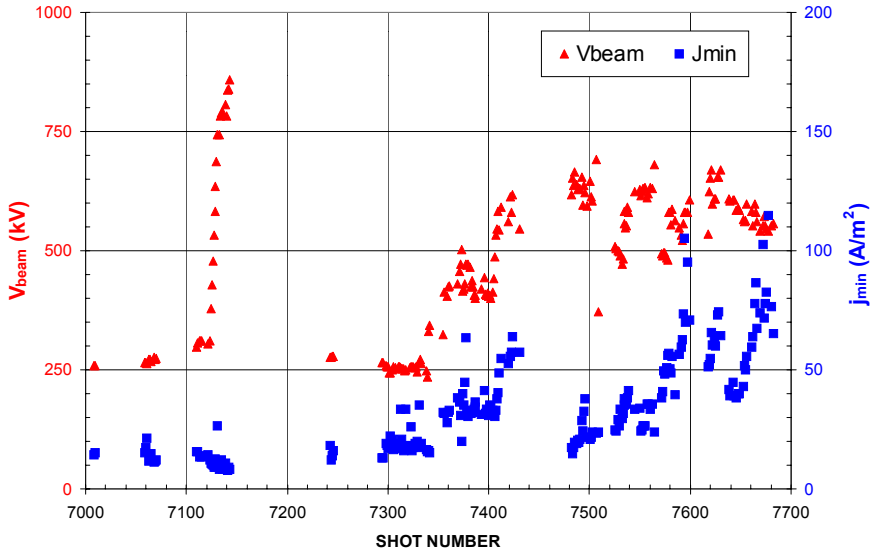

Figure 3 : D⁻ beam energies and current densities for the shots done so far with the "ITER-like" accelerator The current densities in this graph are slightly over evaluated due to slightly different software being used

With the experimental profile information available, we have tried to determine the actual beam optics. If we assume that the starting positions of the beamlets are correct and adjust the steering angles to match the measured positions on the target, the beamlet positions at the target will be correct, but the current density will still be too high. The measured power density indicates that the beamlet optics are worse than those calculated; either the beamlet divergence is higher than calculated, or the beamlet profile not the assumed simple Gaussian. Simply degrading the beamlet divergence to match the peak power density results in calculated profiles that are too narrow at the edge and too wide in the centre (smearing out the individual beamlets). A reasonable match can be found if it is assumed that the beamlet profile is bi-Gaussian with 60 % with a divergence of ≈ 3 mrad and 40 % with a 7 mrad divergence.

HIGHER BEAM ENERGIES AND CURRENTS

There has been a limited number of shots done so far with the new "ITER-like" accelerator. They are all displayed in figure 3. All shots were done with deuterium. Caesium was gradually introduced to the source from shot number 7280 onward. At the end of the shots shown here we had introduced 1.9 g of Cs. Beam energy of 850 keV was obtained in shot 7143 with a current density of 15 A/m^2.

This shot was done without caesium. Breakdown free shots with Caesium gave beams with an energy of 580 keV and a current density of 85 A/m^2.

CONCLUSIONS

HV conditioning pulses have demonstrated that the ITER-like accelerator can hold 930 kV without breakdowns. D$^-$ beams have been produced at 850 keV with a current density of 15 A/m^2.

A current density of 85 A/m^2 has been achieved at 580 keV. The power is measured calorimetrically on the graphite target.

The first experiments have so far confirmed some aspects of the design of the new ITER-like accelerator, but not all. In particular the experiment data suggest that the beamlets have a bi-Gaussian power density distribution (60% with a divergence of ≈3 mrad and and 40% with a 7 mrad) as opposed to the single Gaussian with 2.5 mrad divergence of the simulation.

The positions of the beamlets relative to each other are correct (within 1 mrad), except the central beamlet, which is almost 3 mrad too high. The reasons for these differences are not yet understood. Further experiments and simulations will be carried out in an attempt to understand the differences between the calculated and experimental beam profiles and the accelerated current density.

REFERENCES

[1] L. Svensson, D. Boilson, H.P.L. de Esch, R.S. Hemsworth, A. Krylov and P. Massmann - 22nd SOFT, Helsinki, 2002.

[2] H.P.L. de Esch, R.S. Hemsworth and P. Massmann - Updated physics design ITER-SINGAP accelerator, submitted to Fusion Engineering and Design.

[3] P. Massmann, L. Svensson, H.P.L. de Esch and R.S. Hemsworth - Design and fabrication of the "ITER-like" D⁻ acceleration system, to be presented at 23rd SOFT Venice, 2004.

[4] A. Simonin, G. Delogu, C. Desgranges, M. Fumelli, RSI 70 (1999) 4542.

[5] Y. Okumura - Advanced Negative Ion Beam Technology to Improve the System Efficiency of Neutral Beam Injectors, 18th International Conference on Fusion Energy, Sorrento, Italy, 4-10 October 2000.

[6] P. Massmann, D. Boilson, H.P.L. de Esch, R.S. Hemsworth and L. Svensson - 20th ISDEIV - Tours, 2002.

[7] A. Krylov, R.S. Hemsworth - Gas losses and related beam losses in the ITER NBI, submitted to Fusion Engineering and Design.

REPORTS AND PUBLICATIONS

Experimental results with the new ITER-like 1 MV SINGAP accelerator - L. Svensson, D. Boilson, H.P.L. de Esch, R.S. Hemsworth and P. Massmann - 10th International Symposium on the Production and Neutralization of Negative Ions and Beams, Kiev, 13-17 September 2004.

Design and Fabrication of the "ITER-like" SINGAP D^- Acceleration System – P. Massmann, L. Svensson, H.P.L. de Esch and R.S. Hemsworth - 23rd symposium of fusion technology 20-24 September 2004.

TASK LEADER

Lennart SVENSSON

DRFC/SCCP/GIDEA
CEA-Cadarache
F-13108 Saint-Paul-Lez-Durance Cedex

Tél. : 33 4 42 25 61 69
Fax : 33 4 42 25 62 33

E-mail : lennart.svensson@cea.fr

CEFDA03-1129

Task Title: TW3-TPHI-ICRDES1: ITER ICRF ANTENNA AND MATCHING SYSTEM DESIGN

INTRODUCTION

The elements of the ITER Ion Cyclotron array described in the ITER Reference Design are a modification of the Tore Supra antenna concept (figure 1a), aimed to obtaining resilience to fast resistive load variations, such as those due to ELMs [1]. In figure 1b) it is shown that the in the modified structure, hereafter referred to as ITER-like structure (ILS), unlike in the original one, the input Voltage Standing Wave Ratio (VSWR) can be limited below a specific value, independent of resistive load variations, which depends on the circuit input resistance R_0.

The basic element of the array consists of 2 short-circuited current straps, connected to a tuning network, in series with two variable capacitive reactances, connected in parallel to the input of a RF power source, via a step-up impedance transformer.

The circuit resilience to load variations arises, in part, from the fact that the input admittances of the two sections are complex conjugate, and their imaginary parts cancel out when paralled.

In a dense array, such as the ITER Ion Cyclotron array, (figure 2) a certain level of non conductive (i.e. inductive, and to less extent, capacitive) direct coupling between array elements is present at the plasma end, and most of all, an apparent inter element reactive and resistive coupling is reflected by the plasma load, back to the exciting array elements. It has been suggested [2] that inter-strap coupling in the ITER array would impair the overall load resilience of the proposed array.

2004 ACTIVITIES

EFFECTS OF COUPLING AND LOAD ASYMMETRIES ON LOAD RESILIENCE

In this paper it is shown that full load resilience and perfect impedance match can be preserved by the closed-loop control of the ILS currents.

It is also shown that, in any case, for a predictable behaviour of the ITER array, all array current *must* be controlled, and this should be performed around symmetry conditions that *must* be automatically preserved against unpredictable load variations (due to plasma and random breakdown conditions) to optimize the radiation spectrum, and to avoid control instabilities. If control is lost, the power level of the array must be very rapidly stopped, to prevent equipment damage.

Finally it shown that the ITER array operation is possible, with the hardware described in the ITER Reference Design, and with a suitable array control and protection system, for reasonable assumption on the range of parameter in ITER operation.:
More in detail it is also shown that:

1. An arbitrarily loaded ITER like structure, described by an arbitrary impedance matrix :

$$Z_L = \begin{pmatrix} R_{s1} + 1i \cdot X_{s1} & R_{m2} + 1i \cdot X_{m2} \\ R_{m1} + 1i \cdot X_{m1} & R_{s2} + 1i \cdot X_{s2} \end{pmatrix}$$

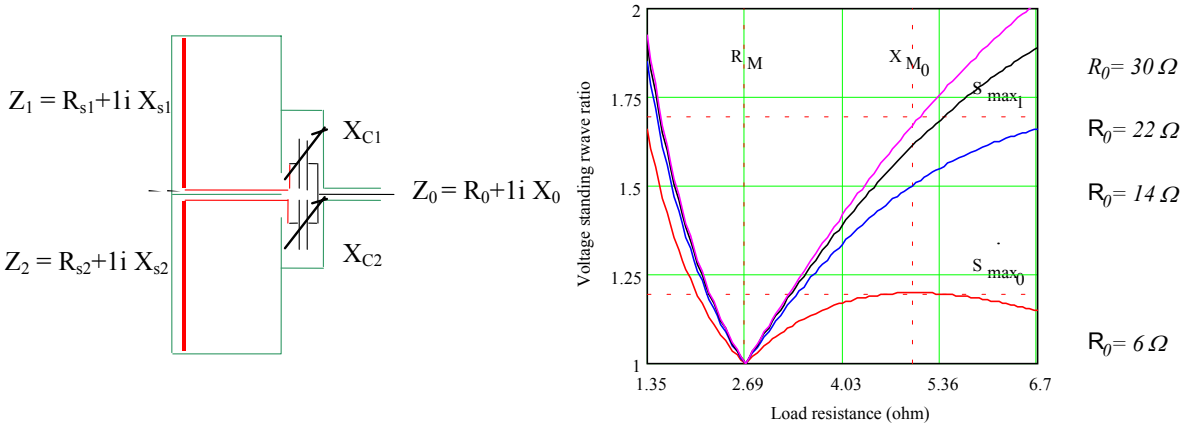

Figure 1 : a) layout of the ITER like structure with tuning element in series, b) Input VSWR as function of load resistance

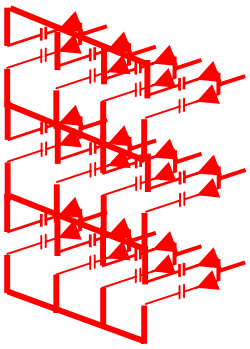

Figure 2 : Sketch of the IC array according to a recent CEA proposal

2. Can be matched to any resistive input impedance R_0, within the limits acceptable to high power sources (VSWR < 1.5), while preserving full load resilience. The number of circuit elements necessary for tuning depends on the level of coupling between the two ILS half sections and on the amount of asymmetry in the diagonal terms of the matrix, while asymmetry in the non diagonal terms is generally negligible.

3. For reasonable values of the coupling coefficient ($k_p \sim$ -20 dB), and for the ITER antenna parameter range, two elements are sufficient to match the ILS.

4. Load asymmetries, in particular if associated with coupling, further complicates the analysis, but the overall picture does not change if the asymmetry in diagonal terms of the matrix is within 10% of the input resistance R_0.

5. For large values of inter element coupling, four tuning elements are needed to preserve both load resilience and impedance match. This is in general achieved with load dependent RF voltage unbalances in the tuning circuit, which aplay no role in the plama coupling process, but may set a limit to the operation of the array, if its dielectric properties are limited.

6. For a large array of coupled elements, such as the ITER IC array, a tight vectorial control of *all* array currents is mandatory, for a stable and efficient operation, independent of the type of array elements and load resilience. Unpredictable, load dependent and severe control instabilities, leading to suppression of the power flow by the RF protection system(s) may occur if the control is lost.

7. On the other hand, the electrical behaviour of an ILS, in which the currents are controlled in closed loop by the internal tuning system, is predictable, and not different from the one of a single strap, since the vectorial relation between input and strap currents is preserved by feedback.

It can be shown that the input impedance of an individual RL circuit (such as a loaded short-circuited current strap) can be perfectly matched to an arbitrary resistive impedance (such as the one of a RF power source) by two purely reactive elements, one in series and the other in parallel. Linking two straps in a ITER-like structure has always practical advantages compared with individually matched elements, because, in addition to load resilience, even if four matching elements are to be used, they can be physically separated in two sections, one within the resonant part of the circuit and the other in the transmission line. As the first pair already significantly reduces the load VSWR, the second can be located at the generator end, since transmission losses are greatly reduced.

CONTROL AND MATCHING

On control issues, we discuss:

1. A general array control strategy of the array $k_{//}$ spectrum control, including power phase, impedance matching control, also addressing the problem of monitoring, control and system protections

2. A procedure for automatic impedance match acquisition and upholding in vacuum and on plasma.

The automatic impedance matching system of a complex array such as the one of ITER is deeply integrated within the overall control and protection system and its operation and stability depends on most, if not all, system parameters.

At the current level of technology, impedance tuning at the power level relevant to fusion devices still requires the mechanical control of the geometry of actively cooled components using vacuum pressurized gas as dielectrics. At an operating frequency of 60 MHz, typical for ITER, the radiation wavelength is $\lambda = 6$ m. Tuning elements based of transmission line sections are therefore bulky and inconvenient for control purposes.

Dimensions of the tuning components can be reduced, if a combination of line sections and lumped circuit elements are used. This allows the construction of tuning equipment having a faster response, and adequate power performances can be obtained in reduced volumes by increasing the dielectric rigidity of the dielectric medium.

For the design of these components, however, a simple analytic approach is insufficient and an adequate electrical and thermal characterization by FEM analysis should be provided.

In the case of ITER, the geometry of the in-vessel equipment is heavily constrained by environmental conditions due to the need of:

- Minimizing electric field and maximizing the dielectric strength in any point of the system.

- Providing adequate nuclear shielding against neutron fields.

- Implementing in the design an adequate structural hardiness to support large electro-magnetic and gravitational loads, due to plasma disruptions and a sufficient flexibility to accept important differential thermal loads.

- Providing a safe vacuum/tritium confinement.

- Allowing intensive water cooling of all components and support structures.

- Permitting remote handling operation on the system.

- Facilitating Hot Cell maintenance, repairs and dismantling.

- Minimizing waste inventory.

In view of these constraints, a simple electrical description of the array control system is insufficient. A description of geometry and electrical properties of the control components and a detailed explanation of how these integrate in the system is needed.

PROPOSALS FOR UPGRADES FOR THE REFERENCE DESIGN

In the paper the discussion of the matching system is part of a wider context, including recent proposals [3] for an upgrade of the ITER IC Reference Design.

The proposed changes have the purpose of:

- Upgrading the array performance.

- Improving the dielectric strength in most part of the array.

- Greatly simplifying the array layout.

- Facilitating maintenance in Hot Cell and, possibly, in situ.

- Implementing an effective vectorial control of the array currents.

- Providing means for breakdown detection and protection.

The new design includes modifications to:

- Strap layout
- VTL layout
- Tuning components and vacuum feed trough

The geometry of the array is significantly changed compared to previous proposals and this has required a substantial revision of the array electrical analysis.

REPORTS AND PUBLICATIONS

[1] G. Bosia - Fusion Science & Technology - 43 pp. 153-159, (2003).

[2] A. Messiaen - Proc of the 15th Topical Conference on RF Power in Plasmas - AIP CP 694, 142, (2003).

[3] G. Bosia - Proposals for upgrades to the ITER Reference design - CEA CNN/NTT (2004).

TASK LEADER

Giuseppe BOSIA in collaboration with S. BREMOND
L. NICOLAS
K. VULLIEZ

DSM/DRFC/SCCP
CEA-Cadarache
F-13108 Saint-Paul-Lez-Durance Cedex

Tél. : 33 4 42 25 49 22
Fax : 33 4 42 25 62 33

E-mail : giuseppe.bosia@cea.fr

CEFDA02-1003
CEFDA03-1111

Task Title: TW2-TPDS-DIASUP4 and TW3-TPDS-DIASUP1: SUPPORT TO THE ITER DIAGNOSTIC DESIGN

INTRODUCTION

ITER requires an extensive set of diagnostic systems to provide several key functions in support of the design goals that include: protection of the device, input to plasma control systems, evaluation and analysis of plasma performance. The process of adapting the design of the diagnostic systems from the original ITER design in 1998 was begun during the EDA Extension Phase. However, considerable detailed design work remains to optimize the measurement capability of the individual systems and to prepare procurement packages for individual diagnostics.

The overall objective of these tasks is to advance the design of several ITER diagnostic systems for which the EU has developed conceptual designs, to re-evaluate their performance for the most recent analysis of plasma conditions, to provide support for the ITER IT in the preparation of the relevant ITER documentation and in evaluating the cost.

These studies have been carried out under two contracts: CEFDA02-1003 signed in August 2003 and CEFDA03-1111 signed in April 2004. However, the technical scope and completion dates of the second contract were modified in a supplementary agreement, signed in Brussels on 31 December 2004, to reflect the revised emphasis of the expected European contribution to ITER diagnostics. The main changes were to cancel a further study that had been planned for polarimetry, to change the focus of the reflectometer study onto the plasma position system and to extend the scope of the other studies. Studies covered by the first contract were completed during 2004 but studies under the second contract, because of the revisions to its technical content and the extension of the completion dates, will extend into 2005. The work involves studies of the following diagnostic systems.

BOLOMETRY

The first phase of this study agreed, in collaboration with the ITER IT, a generic design for the bolometer camera and carried out analysis of the thermal response, defined the cooling requirements and assessed the sensitivity of the bolometer. The second phase (carried out in collaboration with the HAS and IPP fusion Associations) is advancing a number of design and integration issues concerning ITER bolometers. CEA's main contribution is to perform a detailed design analysis of the bolometer camera housing and the internal camera structure for several different camera locations in the ITER vessel.

The study also involves optimization of the camera collimator designs and preliminary assessments of various technical issues including connectors and cables.

THERMOGRAPHY

The study has developed a conceptual design for thermographic measurements in the ITER divertor region based on a novel method using optical fibres (figure 1).

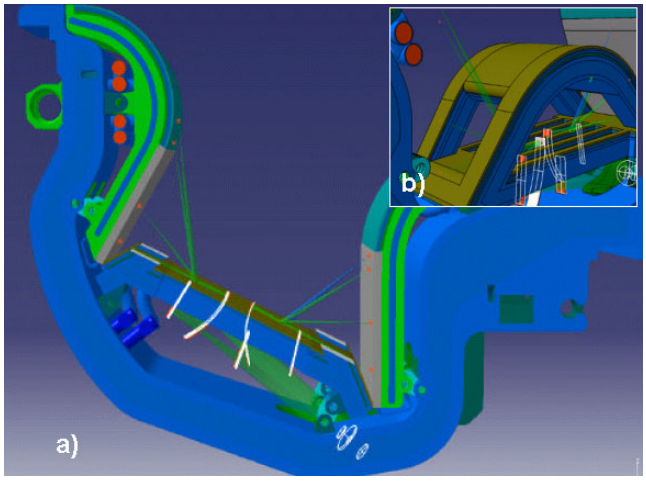

Figure 1 : Thermography diagnostic system for ITER divertor - a) Side view in 3D of optical design implanted in the divertor cassette - b) Passage of inner target viewing lines through dome window

POLARIMETRY

CEA has contributed to a collaborative study led by the FOM Fusion Association. CEA's specific role has been to characterize the change of optical performance in the infrared region of the spectrum of a corner cube reflector when exposed to plasma. This work is linked to the ITER first mirror studies that are described elsewhere in this report.

MOTIONAL STARK EFFECT

This collaborative study was led by CEA and involved also the FOM, UKAEA and VR fusion Associations. CEA's contribution was to perform an initial feasibility study of the possibility of diagnosing the current density profile in ITER by means of the Motional Stark Effect (MSE) using the ITER heating beams. One area of particular importance was to determine the feasibility of MSE at high Lorenz electric field and the CEA study concluded that this is possible. The overall conclusion is that most of the difficulties foreseen with MSE on ITER can be resolved.

WIDE-ANGLE VIEWING

This is a new collaborative study, led by CEA and involving the ENEA and FOM Associations, to perform a design analysis of the optical layouts of the ITER wide-angle viewing systems, with particular emphasis on the systems to be installed on the main horizontal ports. The wide-angle plasma viewing system is an extensive and complex diagnostic with as many as 18 cameras. The original specification, based on a study from the original ITER design in 1998, needs to be brought up to date to take account of recent changes in the ITER design and significant advances in the techniques and expertise for this diagnostic method. An important issue is to assess the extent to which this diagnostic system can complement or even replace other systems.

CALORIMETRY

CEA has carried out an initial study of the feasibility of a diagnostic system for fusion power based on calorimetric measurements of the ITER machine cooling systems.

Q-PROFILE DETERMINATION

This is a 2-part study with the DCU Association (University College Cork) responsible for the first stage and CEA for the second stage. The CEA study has provided expert advice on the determination of MSE measurements in ITER with particular emphasis on the optimization and number of MSE viewing lines and channels.

REFLECTOMETRY

CEA is participating in a collaborative design study (led by the IST Fusion Association) of the plasma position reflectometer systems for ITER. CEA is assessing an existing design for the antenna and estimating antenna loss over the relevant frequency range. CEA is contributing also to the performance analysis of waveguides.

CONCLUSION

Studies covered by the EFDA02-1003 contact are completed: generic design for the bolometer camera [1], conceptual design for thermographic measurements [2], optical performance of the polarimeter system [3], feasibility study of the possibility of diagnosing the current density profile in ITER by means of the Motional Stark Effect [4].

Tasks under the EFDA03-1111 are running according to the revised planning agreed in December 2004.

REPORTS AND PUBLICATIONS

[1] Thermal analysis of the ITER reference bolometers, Final report - DIAG/NTT-2004.027, 10/2004.

[2] Preliminary final report for the EFDA task TWP2002 TW2-TPDS-DIASUP-231 concerning task 2.3 Thermography - part II : CEA, 12/2004.

[3] Support of the ITER Diagnostic design : Polarimetry - Final report - DIAG/NTT 2005-003, 01/2005.

[4] Design analysis of motional stark effect diagnostic for ITER - DIAG/NTT-2004.029, 11/2004.

TASK LEADER

Peter STOTT

DSM/DRFC/SCCP/GCBD
CEA-Cadarache
F-13108 Saint-Paul-Lez-Durance Cedex

Tél. : 33 4 42 25 66 94
Fax : 33 4 42 25 62 33

E-mail : peter.stott@cea.fr

TW2-TPDS-DIADEV-D02

Task Title: DEVELOPMENT OF DIAGNOSTIC COMPONENTS FIRST MIRROR STUDY

INTRODUCTION

First mirrors will be the plasma facing components of optical diagnostic systems in ITER. Attention is concentrated on two processes, which can lead to degradation of mirror optical properties, namely:

- sputtering by charge exchange (CX) neutrals and ions during plasma operation and conditioning procedures such as discharge cleaning, which leads to erosion;
- deposition of material eroded from the divertor (e.g., limiters in TS) and first wall, which leads to surface contamination [1]. In the frame of an EFDA contract, metallic mirror samples (22 mm in diameter, 4 mm thick) of three different materials- mono-crystalline molybdenum (mc-Mo), polycrystalline stainless steel (SS) and copper (Cu) - were installed in TS for long-term plasma exposure during the experimental campaign 2003-2004 [2]. The task included also post exposure mirror analysis. The final report has been delivered according the due date (end 2004).

2004 ACTIVITIES

OPERATION CONDITION

Mirror materials and the experimental layout of mirror exposure have been described in Technofusion 2003.

During the roughly one year exposure period, about 1400 plasma pulses (mainly D_2) of more than Ip = 200 kA (n_{e0} ~ 2-4 10^{19} m^{-3}) have been performed with a cumulative pulse length of ~ 26000 s (7 h 10). The accumulation of injected energy in TS between March 2003 and April 2004 was roughly 37 Gigajoules (GJ) composed of ~ 13 GJ ohmic, ~ 22 GJ lower hybrid and ~ 2 GJ ICRH. In addition wall conditioning procedures of glow discharges in He (t = 362 h, I = 7 μA/cm²; Ua = 300 V, p = 0.3 Pa), in D_2 (t = 606 h, I = 7μA/cm², Ua = 400 V, p = 0.3 Pa) and 13 h of boronisation, alternating with plasma operation, have been performed during this exposure time. A major water leak of an actively cooled in-vessel component in September 2003 led to local mirror "splashing" (the mirrors have not been cleaned after that, before further exposure).

POST EXPOSURE MIRROR ANALYSES

Surface roughness and 3D surface profiles have been measured by confocal microscopy (CM). Surface topography and chemical analyses were performed by SEM imaging, EDX, XPS and SIMS.

Reflectivity measurements were carried out using a spectrophotometer equipped with an integrating sphere operating in the spectral range of 250-2500 nm. Optical constants n (refraction index) and k (extinction coefficient) were measured by ellipsometry in the range between 300-850 nm. All measurements were compared with results obtained on virgin reference samples.

Mc-molybdenum (A-D, B-D)

The surface roughness of the mc-molybdenum samples showed nearly no deterioration (Ra ~ 0.7 nm) and, within the accuracy of the CM measurement method, a net-erosion depth of roughly 0.12 μm. SEM imaging revealed an almost unchanged surface aspect. Some not regular shaped microparticle structures on the surface can be seen; their density is similar than on SS but lower than on Cu surfaces. The elongated form of the particles may indicate shaping by water drops due to an in-situ water leak ("splashing"), which occurred during sample exposition. The composition of these particles measured by EDX is dominated by C and O. XPS measurements on the mirror surface show C1s, Mo 3d, Fe 2p and O 1s lines. The molybdenum line shows a triplet revealing the presence of the bulk material coated with a thin molybdenum trioxide layer (the mirror samples were air exposed after removal from TS). SIMS surface analyses show carbon deposits enriched with hydrogen, deuterium, boron and oxygen (figure 1).

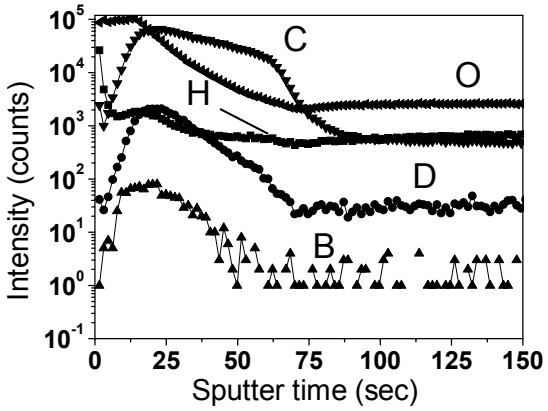

Figure 1 : SIMS spectrum of mc-molybdenum (A-D) mirror sample exposed in TS

In order to estimate the deposited film thickness on the exposed mc-Mo mirror sample, the SIMS facility was calibrated using a Dektak-6M mechanical profiler. A carbon deposit thickness of 12 nm was estimated. This thickness is also in some way confirmed by colorimetry: 10-15 nm thick deposits are still transparent, but 20-25 nm thick ones can be already seen by the unaided eye [3].

The total and the specular reflectivity show a slight decrease compared to the virgin sample. Specular values are compared to SS and Cu in figure 2. This decrease is more pronounced in the UV region. The diffuse reflectivity remains very low (< 2 %). Since the diffusive component of the reflectivity is linked to the roughness of the material, we can deduce that the roughness has not evolved sensibly during exposure (plasma and conditioning procedures), which has been confirmed by surface roughness measurements. We can assume that the decrease of the specular reflectivity is due to light absorption in the thin layer of carbon deposited.

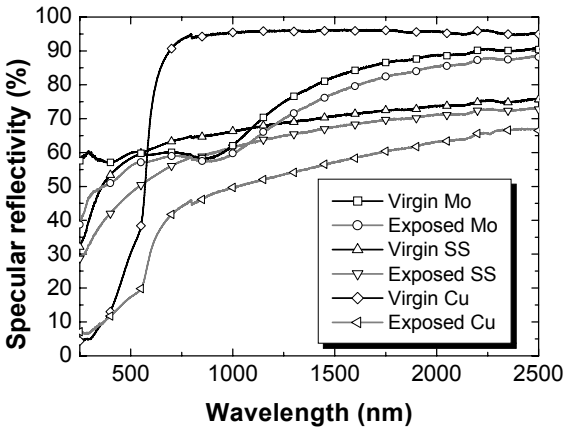

Figure 2 : Specular reflectivity versus wavelength of exposed (mc-Mo, SS, Cu) and virgin reference samples

Stainless steel (A-B, B-B)

The exposed stainless steel sample showed a Ra of 5.7 nm (however, virgin reference samples varied between 1.6 to 8 nm) and a net-erosion depth of roughly 0.22 µm.

A low scale grain-to-grain relief and in-grain topography is visible in SEM. The density of microparticles for the SS surface is similar to that for the Mo sample and, therefore, lower as for Cu. Again the composition of these particles is dominated by C and O. Traces of other impurities such as Mo and Si are observed. SIMS analyses of the mirrors show surface contaminations with oxygen and boron impurities. Also hydrogen and deuterium is observed.

A decrease of both, the total and specular reflectivity (figure 4), is observed after exposure. Diffuse reflectivity is higher especially in the UV region (< 6 %). While SIMS analyses do not allow us to make solid conclusions of the existence of a deposited layer, results from former simulation experiments [1] showed, that such a small erosion depth (~ 0.22 µm) cannot lead to a significant reflectance drop as observed.

Copper (A-G, B-G)

The most dramatic surface aspect change, which is clearly visible by the unaided eye, were observed on the copper mirrors with Ra of 47 and 69 nm, respectively (virgin reference sample varied between 7 to 8 nm) and an important net-erosion depth of roughly 2.6 and 2.33 µm, respectively (figure 3).

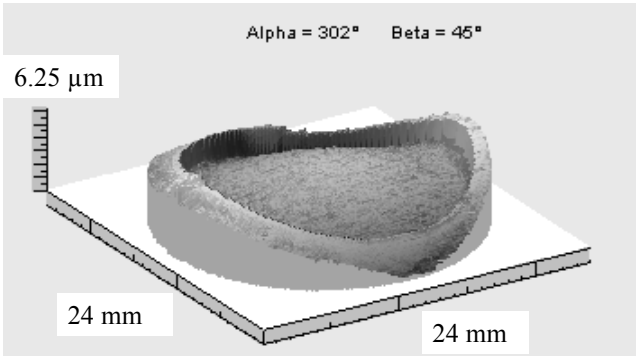

Figure 3 : Confocal microscopy synthesised 3 D image of exposed copper (A-G) mirror sample of 22 mm in diameter

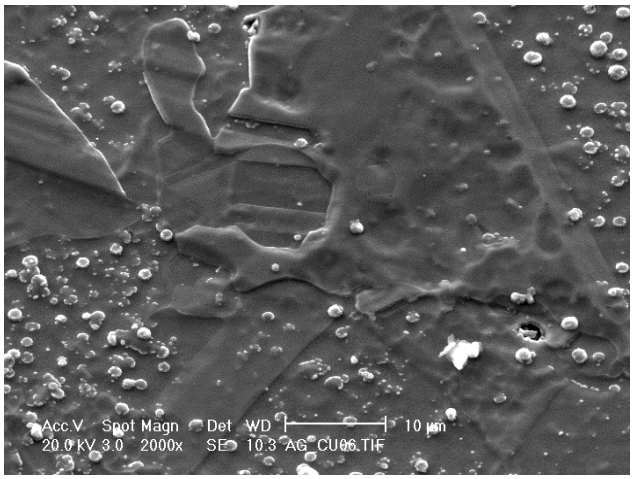

Figure 4 : SEM image of exposed copper (A-G) mirror sample

A strong grain-to-grain relief and in-grain topography is visible in SEM. The grain-to-grain steps seems to be weakened by a deposited layer, which shows an additional erosion topography. The original topography has drastically changed (figure 4). The microparticle density is much higher than for Mo and SS specimens, very different in form and size and depends on grain orientation. The composition of some of these particles with size up to 1 µm is dominated by C and O. XPS spectra show impurities like carbon, boron, silicon and oxygen. Moreover a fitting procedure applied to the copper line reveals the presence of a layer of copper oxide.

Copper is present in two states, as an oxide layer and as a bulk non-oxidized material (the mirror samples were also air exposed after removal from TS). SIMS analyses at the mirror center show contaminations with oxygen and boron impurities. Also hydrogen and a small amount of deuterium can be distinguished. However, these analyses cannot provide us with firm conclusions on the existence of a deposited layer.

The diffuse reflectivity reaches extreme values of about 50 % and, consequently, the specular component ~ 40 % at 800 nm. Therefore, we can assume that the drop of specular reflectivity is mainly due to erosion processes. As for the other mirror materials, relative reflectivity measurements in the FIR (119 µm) showed no significant modifications after exposure.

GLOW DISCHARGE EXPERIMENTS

Mirrors have endured during the one year exposure in TS, conditioning procedures by means of alternating (between plasma operation) glow discharges. In order to verify the influence of erosion due to physical sputtering by ions, virgin reference mirror samples of the same fabrication batch have been exposed ex-vessel to He (t = 402 h, I = 9 μA/cm², Ua = 300 V, p = 1.5 Pa) and D_2 ions (t = 214 h, I = 9 μA/cm², Ua = 400 V, p = 1.5 Pa) in a special laboratory equipment. After each (He and additional D_2) exposure period, surface roughness and profile measurements were performed by CM. From the synthesized 3D images it can be seen that the eroded surface of (TS and ex-vessel) exposed mirrors is not homogeneous and has no rotational symmetry, which complicates, in general, the interpretation of erosion depth. Note, that the mentioned erosion depths are obtained between the exposed mirror border and its shadowed area and, therefore, may not represent correctly an average value. A variety of effects may have led to erosion pattern inhomogeneities, such as: original surface imprecisions, field potential inhomogeneities, particle incidence ("configuration factor"), surface roughness, etc. The laboratory (ex-vessel) results normalized for TS conditioning procedures (exposure time, current density) are in good agreement with TS global net-erosion for Cu, while SS and Mo values diverge up to a factor of 2-3 (table 1). Nevertheless these results show, that erosion due to conditioning procedures is important.

NUMERICAL SIMULATIONS

Numerical simulations were undertaken to characterize the plasma near the mirror samples exposed in Tore Supra, in terms of particle fluxes and energies. The effort was divided into two tasks, assuming that erosion will primarily be caused by CXS neutrals, which are dominant over ion fluxes from the plasma by two orders of magnitude, and deposits formed by carbon eroded and re-deposited from the TPL (toroidal pump limiter):

a) Simulations with the 3-D Monte Carlo code EIRENE have been carried out to calculate the CXS fluxes near the samples.

b) A model describing carbon erosion and re-deposition processes in the Tore Supra CIEL geometry using the BBQ 3-D Monte Carlo scrape-off layer impurity transport code coupled to a core radial impurity transport code (ITC / SANCO / MIST) has been developed, allowing to estimate the expected carbon deposition on the mirror samples.

It was found during the simulation of the plasma conditions, that at the mirror location the CXS and carbon fluxes are minimized due to the geometry of the TS CIEL configuration, thus also minimizing the effect of erosion and deposition during plasma operation. Glow discharges, used for wall conditioning, on the contrary are more or less homogeneous, and their effect is more important at the sample location than the plasma (also due to the long duration of conditioning compared to plasma operation).

The current status of the BBQ simulations allows to give an indication of the order of magnitude for the carbon deposition (0.086 μm). But the interplay of erosion/deposition and the complex sequence of events (plasma operation, glows, leak) makes it extremely difficult to simulate the exact progression of the erosion. However the tendency of calculation results confirm the experimental measurements in the sense, that erosion due to physical sputtering by ions during conditioning procedures dominates over erosion from CX neutrals during plasma operation (table 1).

Table 1 : Comparison between measured (CM) laboratory (ex-vessel) erosion results normalized for TS conditioning procedures (current density, exposure time), TS net-erosion and erosion values from numerical simulations

Exposed mirror sample material	Normalized He (362 h) glow-erosion (μm)	Normalized He (362 h) + D_2 (606 h) glow-erosion (μm)	Net-erosion in TS (μm)	Erosion (num. simul.) plasma + glows (μm)
Mc-Molybdenum	~0.061	0.061+0.25 = 0.31	~0.12	0.107
Stainless Steel	~0.3	0.3 +0.17 = 0.47	~0.22	0.5185
Copper OFHC	~0.31	0.31 +2.53 = 2.84	~2.68	1.008

CONCLUSIONS

The long-term plasma exposure experiment of mirror samples in Tore Supra clearly demonstrate, that the mirror optical properties were degraded due to two opposite processes: (i) deposition of contaminating films (on Mo samples), which are, however, difficult to detect on SS and Cu, (ii) sputtering by CX neutrals during plasma operation and especially ions during alternating long lasting conditioning procedures. The simultaneous demonstration of opposite processes, such as erosion/contamination-deposition observed during mirror exposure in TS suggest, that periods of time when sputtering predominates over deposition (during long lasting glow discharge procedures) and, on the contrary, deposition predominates over sputtering (during plasma operation), having been alternated. Erosion due to physical sputtering by ions during glow discharge procedures in TS was important.

REFERENCES

[1] V. Voitsenya, A. Costley, V. Bandourko, et al., Diagnostic first mirrors for burning plasma experiments, Rev. Sci. Instr. 72 (2001) 475.

[3] P. Wienhold et al., Nucl. Instr. and Meth. in Phys. Res. B 94, (1994), 503-510.

REPORTS AND PUBLICATIONS

[2] M. Lipa, B. Schunke, Ch. Gil et al. - First mirror study in Tore Supra - EFDA ref. TW2-TPDS-DIADEV-D02,Final report, January 2005.

TASK LEADER

Manfred LIPA
Beatrix SCHUNKE
Christophe GIL

DSM/DRFC/SIPP
CEA-Cadarache
F-13108 Saint-Paul-Lez-Durance Cedex

Tél. : 33 4 42 25 4658
Fax : 33 4 42 25 49 90

E-mail : lipa@drfc.cad.cea.fr